Application of a specific membrane fouling control enhancer in membrane bioreactor for real municipal wastewater treatment: Sludge characteristics and microbial community

Lijuan Deng[a], Wenshan Guo[a,*], Huu Hao Ngo[a,c], Xiaochang C. Wang[b,c], Yisong Hu[b,c], Rong Chen[b], Dongle Cheng [a], Shengquan Guo[b], Yunyang Cao[b]

[a] Centre for Technology in Water and Wastewater, School of Civil and Environmental Engineering, University of Technology Sydney, NSW 2007, Australia
[b] Key Lab of Northwest Water Resource, Environment and Ecology, MOE, Xi'an University of Architecture and Technology, Xi'an 710055, P.R. China
[c] International Science & Technology Cooperation Center for Urban Alternative Water Resources Development, Xi'an 710055, P.R. China

*Corresponding author, Email: wguo@uts.edu.au (W. Guo); Tel: +61 2 95142739

Abstract

The feasibility of a novel bioflocculant (GemFloc™) for membrane fouling mitigation in membrane bioreactor (MBR) was investigated during real municipal wastewater treatment. When compared to the conventional MBR (CMBR), suspended sludge in the MBR with GemFloc™ (G-MBR) showed less soluble microbial products (SMP), higher ratios of proteins to polysaccharides in SMP (SMP_P/SMP_C) and loosely bound extracellular polymeric substances (LB-EPS). Adding GemFloc™ also enlarged floc size (> 200 μm), and increased tightly bound EPS levels, zeta potential and relative hydrophobicity of sludge flocs, further reduced cake layer and pore blocking resistances. Moreover, more diverse microbial community and enrichment of fouling reduction microbes such as *Arenimonas*

and *Flavihumibacter* were observed in the G-MBR, together with less abundant microbes (e.g. *Sphaerotilus* and *Povalibacter*) which could aggravate membrane fouling. Therefore, GemFloc™ has high capability in improving sludge characteristics, mitigating membrane fouling and increasing diversity of special functional bacterial community in MBR.

Keywords: Submerged membrane bioreactor (MBR); Bioflocculant; Real wastewater treatment; Membrane fouling control; Microbial community

1. Introduction

Membrane bioreactor (MBR) has been popularly used for treatment and reclamation of various types of wastewater (e.g. municipal wastewater, industrial wastewater, domestic wastewater) since it possesses compact nature (less footprint), ensures high-quality effluent, has capability in resisting high organic loading, generates largely disinfected effluent, and limits sludge generation (Zhang et al., 2019). However, membrane fouling is the major obstacle inhibiting wide application of MBR. Therefore, it is necessary to develop effective strategy to alleviate membrane fouling.

Coagulation/flocculation as an effective treatment approach with various types of flocculants has been employed for membrane fouling mitigation in MBR. Inorganic flocculants, especially ferric based flocculants (e.g. $FeCl_3 \cdot 6H_2O$, $Fe_2(SO_4)_3 \cdot 5H_2O$, $FeClSO_4$, etc.), could enhance sludge filterability, reduce reversible fouling, and ameliorate irreversible fouling by removing soluble microbial products (SMP), leading to greater transmembrane pressure (TMP) decline (Gkotsis et al., 2017). Huang et al. (2019) explored

the feasibility of ferric hydroxide in membrane fouling mitigation in MBR during pharmaceutical wastewater treatment. After adding ferric hydroxide into MBR (Fe-MBR), the amount of larger biomass flocs increased through neutralizing negatively surface charge of activated sludge compared to a control MBR (co-MBR). The increase in bacterial activity and significant decline in relative abundance of bacteria contributing to biofilm formation (e.g. *α-proteobacteria*, *β-proteobacteria*, *Flavobacteriia*) reduced dissolved organic matters (DOMs) in SMP (e.g. dissolved organic carbon, carbohydrate, low molecular weight compounds and biopolymer). These effects effectively mitigated membrane fouling in the Fe-MBR (about 35% longer operational duration compared to the Co-MBR). On the other hand, organic flocculants (e.g. biopolymers, cationic polymers, etc.) can not only prolong filtration cycles, but also reduce inorganic elements (e.g. silicon, calcium, magnesium, aluminium, and iron) as well as concentrations of SMP, extracellular polymeric substances (EPS) and colloidal total organic carbon. These flocculants also enlarged mean floc size, which further increased impact resistance and enhanced floc's adaptive capacity to changing environment, resulting in less SMP release (Alkmim et al., 2015; Zhou et al., 2017a).

Nevertheless, inorganic and organic flocculants can exert adverse impact on environment and human health, and may generate 'secondary pollutants' (e.g. metals, toxic sludge, acrylamide oligomers, etc.) during wastewater reclamation and reuse processes (Mateus et al., 2017). Therefore, bioflocculants or natural flocculants have been developed and used for fouling alleviation due to less ecological and health impact. Tan et al. (2017) employed salt-tolerant *Arthrobacter* as a kind of bioflocculants and slower membrane fouling development was observed in MBR when treating saline wastewater. The

bioflocculation by *Arthrobacter* not only facilitated the reduction of fouling-related components (e.g. EPS in sludge, SMP in supernatant solution), but also decreased the humic acid-like, fulvic acid-like and aromatic proteins components (large biomolecules). Modified starches (e.g. MGMS, CGMS) could remarkably reduce gel and cake resistances as well as concentrations of macromolecules with molecular weight (MW) ≥ 100 kDa in supernatant of MBR. Compared with MGMS, the addition of CGMS in MBR (CGMS-MBR) generated larger-size sludge flocs with lower fractal dimension, thus increasing porosity of fouling layer. It also prompted detachment of flocs from membrane surface, leading to lower fouling rate in the CGMS-MBR (Ji et al., 2015).

Our previous studies used a new green bioflocculant in MBR for synthetic domestic wastewater treatment. Compared to the conventional MBR, the bioflocculant could reduce energy consumption due to less backwash frequency, significantly alleviate membrane fouling (TMP increase of 2.5 kPa during 70 days of operation), improve sludge properties (e.g. less SMP, larger floc size, higher zeta potential, higher relative hydrophobicity) as well as limit cake layer formation and pore blocking (Deng et al., 2015; Ngo and Guo et al., 2009). However, the application of bioflocculant in real wastewater treatment and the resulting changes in microbial community in activated sludge have yet to be explored. Hence, in this study, the performance of two lab-scale MBRs, one with the patented bioflocculant (GemFloc™) developed at University of Technology Sydney and the other without bioflocculant were compared for real municipal wastewater treatment during long-term operation. More specifically, membrane fouling behaviors (TMP and fouling resistance) were evaluated together with sludge characteristics (including mixed liquor

suspended solids (MLSS), mixed liquor volatile suspended solids (MLVSS), zeta potential, relative hydrophobicity (RH), particle size distribution (PSD), EPS and SMP compositions). Given the important role of bacterial population in determining sludge characteristics and membrane fouling behaviors, this paper also analyzed microbial community structure in both MBRs.

2. Materials and methods

2.1. Real wastewater

Real municipal wastewater taken from a local wastewater treatment plant (WWTP), Xian, China was employed as the feed for both MBRs in this study. The real wastewater contains COD_{Cr} of 400-560 mg/L, BOD_5 of 198-236 mg/L, NH_4-N of 26.8-37.2 mg/L, total nitrogen (TN) of 40.2-56.1 mg/L and total phosphorus (TP) of 8.63-11.91 mg/L with pH of 7.52 ± 0.36. pH of MBRs was adjusted by $NaHCO_3$ or H_2SO_4 to a constant value of 7.

2.2. Experimental set-up and operating conditions

Two lab-scale submerged MBRs with same effective working volume of 5 L, including MBR with GemFloc™ addition (G-MBR) and conventional MBR (CMBR), were operated in parallel. The submerged hollow fiber membrane module in MBR was made of polyvinylidene fluoride (PVDF) membrane fibers (Tianjin Motimo Membrane Technology Co., Ltd.) with pore size of 0.03 μm and an effective surface area of 0.12 m^2. Activated sludge in both MBRs was collected from the WWTP and was acclimatized for more than two weeks using real wastewater before starting. Initial mixed liquor suspended sludge concentration was adjusted to around 5.0 g/L in both MBRs. During the experimental

117 period, sludge was not discharged to obtain infinite sludge retention time (SRT).
118 GemFloc™ dosage in the G-MBR was 0.5 g/d. The suction pump was employed to
119 withdraw permeate from the membrane module at a constant filtration flux of 8 $L/m^2 \cdot h$.
120 Thus the hydraulic retention time (HRT) amounted to 5.21 h. An air diffuser placed below
121 the membrane module was employed to supply aeration from an air compressor. The air
122 flow rate was kept at 2.5 L/min. Periodical backwash at two times per day was adopted to
123 physically clean membrane. When TMP reached above 35.0 kPa, off-line chemical
124 membrane cleaning was conducted by immersing the membrane module in 0.8% (w/w)
125 hydrochloric acid for 8 h, followed by 0.9% (w/w) sodium hypochlorite for 8 h and finally
126 0.4% (w/w) sodium hydroxide for 8 h.
127
128 **2.3. Analysis methods**
129 Measurements of MLSS and MLVSS were conducted according to the standard
130 methods (APHA et al., 1998). The standard methods (APHA et al., 1998) were also
131 adopted for determination of chemical oxygen demand (COD), ammonia (NH_4-N), nitrite
132 (NO_2-N), nitrate (NO_3-N) and phosphorus (PO_4-P) concentrations of influent and effluent
133 by employing a HACH DR6000 UV VIS spectrophotometer (HACH Co., USA). Sludge
134 volume index (SVI) of suspended sludge was gauged in a 1000 mL graduated cylinder.
135 Sludge samples were centrifuged at 3000 rpm for 30 min to obtain supernatant, which was
136 centrifuged again and further filtered through 0.45 μm syringe filter. The final solution was
137 collected as soluble microbial products (SMP) (Deng et al., 2015). According to Chen et al.
138 (2017a), the sludge pellets in the centrifuge tube were re-suspended in 0.05% NaCl

139 solution, followed by being sonicated at 20 kHz for 2 min, shaken at 150 rpm for 10 min,
140 sonicated again, and centrifuged at 8,000 *g* for 10 min to get the supernatant for loosely
141 bound extracellular polymeric substances (LB-EPS). Extraction of supernatant for tightly
142 bound extracellular polymeric substances (TB-EPS) was carried out by re-suspending
143 sludge pellet left in the centrifuge tube in 0.05% NaCl solution, which was further
144 sonicated at 20 kHz for 3 min, heated at 60 ºC for 30 min and centrifuged at 12,000 *g* for 20
145 min to collect the supernatant. The aforementioned supernatants were filtered through 0.45
146 μm syringe filter to obtain LB-EPS and TB-EPS. Proteins ($LB\text{-}EPS_P$, $TB\text{-}EPS_P$ and SMP_P)
147 and polysaccharides ($LB\text{-}EPS_C$, $TB\text{-}EPS_C$ and SMP_C) in extracted samples were analysed
148 by modified Lowery method (Sigma, Australia) and Anthrone-sulphuric acid method,
149 respectively. Concentrations of proteins and polysaccharides were finally determined by the
150 above-mentioned HACH spectrophotometer. A zeta potential meter (Zetasizer Nano ZS,
151 Malvern Instrument, UK) was used for determining zeta potential of mixed liquor. The
152 relative hydrophobicity (RH) of sludge flocs was analysed based on the protocol proposed
153 by one of our previous studies (Deng et al., 2015). The determination of particle size
154 distribution of sludge flocs was conducted using a laser granulometer (Mastersizer 2000,
155 Malvern Instruments, UK).

156 After terminating the experiment at TMP above 35 kPa, resistance-in-series model and
157 Darcy's equations were applied to determine membrane filtration characteristics (Choo and
158 Lee, 1996):

159 $$J = \Delta P/\mu R_T \quad (1)$$

160 $$R_T = R_M + R_C + R_P \quad (2)$$

where J is the permeate flux, ΔP is the TMP, μ is the viscosity of the permeate, R_T is total resistance, R_M is the intrinsic membrane resistance, R_C is the cake resistance, and R_P is the pore blocking resistance.

The bacterial community structure of suspended sludge samples were analysed by Sangon Biotech in China using high-throughput sequencing.

3. Results and discussion

3.1. Organic and nutrient removals

Both of the G-MBR and the CMBR showed good COD removal of 96.25 ± 7.81% and 90.36 ± 8.36%, respectively, implying slightly enhanced organic matter removal by application of the bioflocculant. Although small difference in NH_4-N removal was observed between the G-MBR (90.67 ± 6.82%) and the CMBR (85.72 ± 8.45%), the G-MBR demonstrated greater TN removal (80.36 ± 5.12%) compared to the CMBR (37.75 ± 7.24%). It was ascribed to that the retention of nitrifying bacteria by the membrane in both MBRs led to high degree of biological nitrification. When compared with the CMBR, the presence of larger flocs in the G-MBR might facilitate the formation of anoxic/anerobic microenvironment at the inner layer of the flocs. Better TN removal in the G-MBR could be due to the occurrence of oxygen gradient inside these larger flocs (see Section 3.2) despite of high DO levels (5.0-7.0 mg/L). The addition of GemFloc™ could also improve the accumulation of phosphorus accumulating organisms (PAOs) and biomass metabolism, which, in turn facilitated enhanced biological phosphorus removal, achieving better PO_4-P removal in the G-MBR (93.61 ± 7.58%) compared to that for the CMBR (59.33 ± 8.96%).

183 More detailed analyses regarding microbial community structure contributing to organic
184 and nutrient removals are presented in Section 3.4.
185
186 **3.2. Membrane fouling behaviors**
187 During the entire study period, TMP of the CMBR exhibited a gradual increment from
188 2.70 to 10.35 kPa within the first 21 days of operation followed by a sharp jump, reaching
189 36.20 kPa on day 30 (Fig. 1). Compared to the CMBR, the G-MBR presented a slower
190 TMP increase from 2.57 to 15.36 kPa before day 51. Subsequently, a remarkable TMP rise
191 was observed and chemical cleaning was implemented until day 58 as TMP exceeded 35
192 kPa (36.68 kPa). It could be inferred that the fouling rate for the CMBR (1.11 kPa/d) was
193 almost two times higher than that for the G-MBR at 0.59 kPa/d. Hence, GemFloc™
194 addition significantly slowed down membrane fouling development, enhanced membrane
195 permeability and extended the operational duration of MBR.
196 **Fig. 1.**
197
198 At the end of experiment, fouling resistance distribution was obtained for both the G-
199 MBR and the CMBR (Table 1). The CMBR exhibited considerably higher total fouling
200 resistance (R_T) than the G-MBR (6.13×10^{12} and 3.73×10^{12} m^{-1}, respectively). GemFloc™
201 addition significantly reduced cake layer resistance (R_C) in the G-MBR by 46.78%,
202 obtaining 2.40×10^{12} m^{-1}. R_C of both MBRs made a great contribution to R_T, accounting for
203 64.34% and 73.57% of R_T for the G-MBR and the CMBR, respectively. Pore blocking
204 resistance (R_P) in the G-MBR (0.17×10^{12} m^{-1}) was about one third of that for the CMBR

205 (0.46×10^{12} m^{-1}). Thus GemFloc™ could effectively retard cake layer formation and pore
206 blocking, thus alleviating membrane fouling.

207 **Table 1.**

208

209 **3.3. Sludge properties**

210 **3.3.1. MLSS concentration**

211 The G-MBR and CMBR possessed initial MLSS concentrations of 4.98 g/L and 5.06
212 g/L, respectively. Since there was no sludge withdrawal during the experiment, continuous
213 growth of suspended biomass occurred, finally reaching 11.62 g/L in the G-MBR on day 58
214 and 11.05 g/L in the CMBR on day 30, which indicated that lower biomass growth rate
215 ($\Delta MLSS/\Delta t$) was obtained due to GemFloc™ addition (0.11 g/L·d) compared to that for the
216 CMBR (0.19 g/L·d). The lower SVI of 71.88-129.89 mL/g for the G-MBR (91.54-151.82
217 mL/g for the CMBR) also implied the denser and heavier settled sludge and better
218 settleability of sludge. MLVSS concentrations ranged from 3.39 to 10.00 g/L and from 3.40
219 to 8.21 g/L in the G-MBR and CMBR, respectively. The obtained higher MLVSS/MLSS
220 ratio in the G-MBR in the range of 0.68-0.86 than that in the CMBR (0.67-0.74) might be
221 owing to the presence of GemFloc™ increased fraction of organic content and reduced
222 biomass mineralization (Krzeminski et al., 2012).

223

224 **3.3.2. Particle size distribution of biomass flocs**

225 In the CMBR, sludge flocs showed a narrow particle size distribution from 0.4 to 600
226 μm. The sludge flocs with size less than 150 μm and larger than 200 μm accounted for

227 about 64% and 21% of total sludge volume, respectively (Fig. 2). During the first 15-day
228 operation, particle size distribution of sludge flocs in the G-MBR was in a wide range of
229 0.4-1300 μm. Small flocs (< 150 μm) and larger flocs (> 200 μm) took 57% and 26% of
230 total sludge volume, respectively. After that, sludge flocs in the G-MBR shifted towards a
231 broader particle size distribution with median particle size larger than 200 μm (50% of total
232 sludge volume) and smaller floc size < 150 μm (38% of total sludge volume). From day 50,
233 the proportion of larger flocs declined but that of small flocs increased, as demonstrated by
234 47% for flocs smaller than 150 μm and 39% for flocs larger 200 μm. Additionally, the floc
235 size range was narrowed to 0.4-800 μm. The decrease in the proportions of large flocs but
236 increase in percentages of small flocs in total sludge volume after 50 days was almost
237 consistent with the trend of TMP development (TMP jump) in the G-MBR. It indicated that
238 serious membrane fouling after 50 days could be partially explained by the increased
239 amounts of small flocs. Nevertheless, the fraction of larger flocs was still higher in the G-
240 MBR than those for the CMBR throughout the whole experiment.
241 **Fig. 2.**
242
243 As particle size of sludge flocs were at least ten times than that of the membrane pore
244 size, the biomass floc size in this study might not be considered as the key factor
245 contributing to pore blocking. Backtransport velocity of sludge flocs with smaller size was
246 smaller due to lower physical forces on the particles (i.e. inertial lift), which increased
247 amount of small flocs in the cake. This further reduced permeability and void fraction of
248 cake layer (Ma et al., 2013). Thus greater proportion of smaller flocs in the CMBR
249 accounted for the increased R_C. On the other hand, GemFloc™ showed its positive and

250 long-term effects on flocculation ability and aggregation of sludge flocs, which favored the
251 formation of larger biomass flocs, leading to formation of more porous and higher
252 permeable cake layer on membrane surface (Park et al., 2006). Consequently, R_C was lower
253 in the G-MBR than that in the CMBR.

254 Compared to those in the CMBR (zeta potential of -18.6 mV – -15.1 mV, relative
255 hydrophobicity (RH) of 32.36% – 42.76%), GemFloc™ addition increased zeta potential (-
256 11.1 mV – -7.25 mV) by neutralizing or reducing negative surface charge of sludge flocs
257 and enhanced sludge hydrophobicity by increasing RH (64.13% – 79.33%) of sludge flocs
258 in the G-MBR. These effects increased flocculation ability of sludge flocs, which was
259 associated with the enlarged floc size of suspended sludge in the G-MBR.

260

261 **3.3.3. EPS and SMP compositions of suspended sludge**

262 At relatively low TMP (< 16 kPa), the CMBR possessed higher levels of total SMP
263 and polysaccharides in SMP (SMP_C) (20.47-55.86 and 9.06-30.18 mg/L, respectively)
264 compared to the G-MBR (14.82-44.09 and 5.33-17.36 mg/L, respectively), corresponding
265 to lower ratios of proteins to polysaccharides (SMP_P/SMP_C) (0.76-1.59 in the CMBR and
266 1.54-2.09 in the G-MBR) (Table 2). When membrane fouling became more serious (TMP
267 16-37 kPa), total SMP remarkably increased in the CMBR (61.18-95.85 mg/L).
268 Additionally, SMP_C showed a notable ascending trend, reaching 32.39-53.67 mg/L. On the
269 other hand, contents of SMP and SMP_C in the G-MBR were lower at 53.12-62.98 and
270 23.76-29.26 mg/L, respectively. Significantly declined SMP_P/SMP_C ratio was detected for
271 the CMBR (0.79-0.89) when compared with that for the G-MBR (1.15-1.24). Greater levels

of SMP aggravated membrane fouling in the CMBR by encouraging membrane pore blocking, formation of gel layer with considerably high specific filtration resistance as well as penetration into spaces between particles and pores in cake layer. Moreover, as polysaccharides contribute to membrane fouling development (especially irreversible fouling) and gel layer formation on membrane surface (Deng et al., 2016), more serious membrane fouling, greater R_P and R_C in the CMBR could be partially ascribed to higher SMP levels and lower SMP_P/SMP_C ratio.

Table 2.

Compared to the G-MBR (LB-EPS of 43.80-123.72 mg/L and $LB\text{-}EPS_P/LB\text{-}EPS_C$ of 1.56-3.14 mg/L, respectively), higher concentrations of LB-EPS and lower ratio of proteins to polysaccharides in LB-EPS ($LB\text{-}EPS_P/LB\text{-}EPS_C$) were detected in the CMBR at different TMP ranges, corresponding to 62.69-180.84 and 0.89-2.06 mg/L, respectively. LB-EPS has highly hydrated matrix, possessing a dispersible and loose slime layer without an obvious edge. Thus the presence of LB-EPS at greater levels induced poor attachment between cells and floc structure, caused the production of highly porous sludge flocs at low density, and deteriorated sludge bioflocculation. This could give rise to poorer settleability of sludge flocs (higher SVI values), larger amount of fine particles and serious membrane fouling in the CMBR (Li and Yang, 2007). Hence higher R_C and R_P in the CMBR were also ascribed to higher LB-EPS levels.

In the G-MBR, the greater $LB\text{-}EPS_P/LB\text{-}EPS_C$ increased zeta potential and RH of sludge flocs as proteins provide the amino groups with positive charge and amino acids with hydrophobic side group, resulting in better flocculation ability of flocs and further

295 favored formation of bigger and more permeable flocs (Zhang et al., 2016). TB-EPS which
296 attaches to peripheral capsules of cell surface favors the aggregation of cells in clusters.
297 The increased TB-EPS levels of activated sludge helped agglomeration of sludge flocs by
298 GemFloc™ addition (85.37-121.93 mg/L for the G-MBR, 67.84-83.61 mg/L for the
299 CMBR), which enlarged flocs in the G-MBR (Chen et al., 2017b). Furthermore, levels of
300 proteins as major components of TB-EPS (TB-EPS_P) were higher in suspended sludge of
301 the G-MBR (54.11-78.26 mg/L) than those for the CMBR (45.36-59.51 mg/L). Proteins
302 could keep bacterial cells together and maintain cell cohesion by forming an active gel-like
303 matrix (Dogsa et al., 2005). Thus more TB-EPS_P in activated sludge also facilitated the
304 formation of larger flocs due to addition of GemFloc™. In the G-MBR, higher LB-
305 EPS_P/LB-EPS_C ratio and TB-EPS_P levels were responsible for the formation of larger flocs.
306

307 **3.4. Microbial community structure at genus level**

308 **3.4.1. Microbial community structure contributing to organic and nutrient removals**

309 Higher proportion of *Phaeodactylibacter* was found in the G-MBR (1.27-3.01%) than
310 that in the CMBR (< 1.21%), which might help to improve organic matter removal by
311 application of GemFloc™ throughout the entire experimental period (Xu et al., 2018).
312 During TMP development in the range of 10-16 kPa, both of the G-MBR and CMBR
313 possessed high relative abundance of nitrifying bacteria, including *Nitrosomonas* (10.88%
314 and 9.54%, respectively) and *Nitrospira* (5.19% and 4.12%, respectively). More abundant
315 denitrifying bacteria (7.92% for *Defluviimonas*, 4.98% for *Pseudolabrys*) and PAOs (1.46%
316 for *Gemmatimonas*) were found due to GemFloc™ addition compared to that in the CMBR

317 (3.52%, 1.32%, and 0.76%, respectively). When TMP reached above 35 kPa, greater
318 abundance of nitrifying bacteria and PAOs were also found in the G-MBR compared to the
319 CMBR (8.36% vs 4.88% for *Nitrosomonas*, 3.27% vs 2.36% for *Nitrospira*, 3.55% vs
320 0.97% for *Gemmatimonas*). The declined ratios of *Nitrosomonas* and *Nitrospira* might be
321 mainly ascribed to that the increase in diversity of microbial population decreased the
322 proportion of nitrifying bacteria in total microbial population. These results could explain
323 better nitrogen and phosphorus removal achieved by GemFloc™ addition (Miao et al.,
324 2015; Zhang et al., 2003; Zhou et al., 2017b).
325
326 **3.4.2. Microbial community structure contributing to membrane fouling**
327 Microbial community structure in the CMBR and G-MBR regarding the
328 microorganisms associated with membrane fouling and sludge characteristics are displayed
329 in Figs. 3 and 4. In the CMBR, majority of microbial population was associated with
330 serious membrane fouling and poor sludge properties. At low TMP (10-16 kPa), great
331 abundance of *Haliscomenobacter* (as one kind of filamentous bacteria, 7.50%) and
332 *Hyphomicrobium* (8.56%) deteriorated sludge settleability and compaction, which might be
333 responsible for the increase of SVI (Gu et al., 2018; Layton et al., 2000). The abundant of
334 another filamentous microbe, namely *Thiothrix* (8.18%), indicated the generation of
335 extracellular polymers (e.g. LB-EPS) and further aggravated membrane fouling (Gao et al.,
336 2014). More LB-EPS_C and more serious membrane fouling could be associated with high
337 abundance of *Bradyrhizobium* (3.62%) which could secrete extracellular polysaccharides
338 (Friha et al., 2014). *Novosphingobium* is normally found in biocake or biofilm and

339 *Chryseolinea* can induce membrane fouling by fermentation of polysaccharides (Matar et
340 al., 2017; Xu et al., 2018). Hence the enrichment of *Novosphingobium* (6.56%) and
341 *Chryseolinea* (5.42%) might be partially relevant to membrane fouling. On the other hand,
342 the microorganisms which are able to degrade membrane fouling-induced substances (e.g.
343 polysaccharides (SMP_C and LB-EPS_C), proteins (SMP_P and LB-EPS_P)) and mitigate
344 membrane fouling were detected at low levels (< 1.60%), including *Reyranella,*
345 *Thermogutta, Tepidisphaera* and *Comamonas*, except for *Pirellula* at 2.74% and *Kofleria* at
346 3.48% (Inaba et al., 2018; Lang et al., 2014; Liu et al., 2018; Peng et al., 2019; Zheng et al.,
347 2019; Zhou et al., 2017b; Zhu et al., 2017). When TMP reached above 35 kPa, serious
348 membrane fouling in the CMBR could be induced by the enrichment of filamentous
349 bacteria such as *Sphaerotilus*, *Thiothrix* and *Haliscomenobacter* at 8.95%, 8.28% and
350 8.16%, respectively. *Sphaerotilus* enables production of large assemblage and more EPS,
351 thus facilitating colonization and biofilm formation on membrane surface (Peng et al.,
352 2019). Moreover, *Thiothrix* and *Haliscomenobacter* also favor generation of extracellular
353 polymers (i.e. LB-EPS) and negatively influence sludge settleability (Gao et al., 2014; Gu
354 et al., 2018). In addition, the presence of high levels of *Novosphingobium*, *Povalibacter* and
355 *Chryseolinea* (7.78%, 6.82% and 6.23%, respectively) might also aggravate membrane
356 fouling (Choi et al., 2017; Matar et al., 2017; Xu et al., 2018). Furthermore, *Acinetobacter*,
357 which is related to the production of extracellular polysaccharides (SMP_C and LB-EPS_C)
358 (Abdel-El-Haleem et al., 2003), was detected at 6.54% at the end of the experiment. Thus
359 membrane fouling was more severe for the CMBR.
360 **Fig. 3**
361 **Fig. 4.**

GemFloc™ addition could enhance the variety of microbial community structure which helped to improve sludge properties and reduce membrane fouling in the G-MBR. The presence of *Terrimonas* positively affects flocculation performance of suspended sludge and promotes aggregation of sludge flocs by secreting extracellular polymers with hydrophobic components (Zhao et al., 2019). *Thauera* favors EPS generation, especially proteins as hydrophobic components contributing to cell aggregation and floc formation (Dong et al., 2017; Zhang et al., 2018). When TMP was low at 10-16 kPa, great abundance of *Terrimonas* and *Thauera* (4.76% and 4.34%, respectively) might contribute to better flocculation ability and aggregation of sludge flocs through generating more TB-EPS_P. *Kofleria* (7.72%), *Pirellula* (5.65%), *Reyranella* (4.14%), *Thermogutta* (2.16%) and *Tepidisphaera* (1.63%) were also responsible for reduced proteins (SMP_P and LB-EPS_P) and polysaccharides (SMP_C and LB-EPS_C). The high hydrophobicity of sludge flocs might be ascribed to the high presence of *Pseudomonas* and *Rhodobacter* (2.74% and 1.41%, respectively) (Chao et al., 2014; Sutherland et al., 2001). After terminating the experiment (TMP > 35 kPa), the abundance of *Kofleria* increased (8.22%), which could explain the evidently less SMP_C and LB-EPS_C, while high levels of *Reyranella* (4.75%) and *Pirellula* (4.32%) led to less SMP_C, SMP_P, LB-EPS_C and LB-EPS_P. In addition, the proportion of *Flavihumibacter* at 4.16% resulted in larger size of sludge flocs via providing structural network during the experiment (Luo et al., 2015). Nevertheless, the decline in *Terrimonas* (4.40%) and *Thauera* (4.26%) might deteriorate flocculation and aggregation ability of suspended sludge to some extent. The microorganisms contained greater abundance of

384 *Thermogutta* (4.03%), which might potentially induce more accumulation of SMP_C and
385 $LB\text{-}EPS_C$. Overall, the abundant *Terrimonas, Thauera* and *Thermogutta* were the main
386 contributor to aggravated membrane fouling in the G-MBR.
387 Compared to the CMBR, the G-MBR contained more abundant bacterial population
388 giving rise to better sludge properties and membrane permeability but less microorganisms
389 aggravating membrane fouling. Additionally, more diverse microbial communities were
390 found in the G-MBR than those in the CMBR, especially at high TMP (> 35 kPa), which
391 also favored fouling control. As an aerobic bacterium, *Arenimonas* can also degrade various
392 sugars and amino acids (Cui et al., 2019). Hence, the presence of *Flavihumibacter*,
393 *Reyranella, Pirellula*, *Thauera, Thermogutta, Arenimonas, Rhodobacter, Comamonas* and
394 *Pseudomonas* in the G-MBR (1.87%-4.75%) was associated with the enhanced sludge
395 properties (i.e. less proteins and polysaccharides, higher hydrophobicity, better sludge
396 aggregation). On the other hand, genera *Povalibacter, Acinetobacter* and *Chryseolinea*
397 were only detected in the CMBR at great abundance (6.23%-6.82%), which were closely
398 linked with the accumulation of SMP_C and $LB\text{-}EPS_C$ and further serious membrane fouling.
399

400 **4. Conclusions**

401 The effectiveness of GemFloc™ on membrane fouling reduction in MBR was
402 evaluated for real municipal wastewater treatment. Compared to the CMBR, GemFloc™
403 could alleviate membrane fouling, reduce SMP and LB-EPS, increase ratio of SMP_P/SMP_C
404 and $LB\text{-}EPS_P/LB\text{-}EPS_C$, enlarge floc size, and increase $TB\text{-}EPS_P$, zeta potential and RH,
405 thus decreasing R_C and R_P. Moreover, GemFloc™ addition induced higher diversity of

406 microbial community and greater abundance of special functional microorganisms (e.g.
407 *Arenimonas*, *Flavihumibacter*), which enhanced sludge properties and alleviated membrane
408 fouling. Thus GemFloc™ could be a promising novel bioflocculant to control membrane
409 fouling.
410

411 **Appendix A. Supplementary data**

412 E-supplementary data associated with this article can be found in the online version.
413

414 **Acknowledgement**

415 This research was supported by the UTS Research Services "Case studies of
416 Gemfloc™ on membrane fouling control in a pilot-scale aerobic MBR system for
417 municipal wastewater treatment towards its full-scale application in China", with AWR
418 Environmental Research Co., Ltd., China (Project ID PRO17-3427). The authors are also
419 grateful for Tianjin Motimo Technology Co., Ltd. for supplying membrane fibers.
420

421 **References**

422 1. Abdel-El-Haleem, D., 2003. *Acinetobacter*: environmental and biotechnological
423 applications. Afr. J. Biotechnol. 2(4), 71–75.
424 2. Alkmim, A.R., da Costa, P.R., Moser, P.B., França Neta, L.S., Santiago, V.M. J.,
425 Cerqueira, A.C., Amaral, M.C.S., 2015. Long-term evaluation of different strategies of
426 cationic polyelectrolyte dosage to control fouling in a membrane bioreactor treating
427 refinery effluent. Environmen. Technol. 37(8), 1026–1035.

3. APHA, AWWA, and WEF, 1998. Standard Methods for the Examination of Water and Wastewater, twentieth ed. American Public Health Association, Washington, DC.
4. Chao, Y., Guo, F., Fang, H.H.P., Zhang, T., 2014. Hydrophobicity of diverse bacterial populations in activated sludge and biofilm revealed by microbial adhesion to hydrocarbons assay and high-throughput sequencing. Colloids Surf. B: Biointerfaces 114, 379–385.
5. Chen, W., Gao, X., Xu, H., Cai, Y., Cui, J., 2017a. Influence of extracellular polymeric substances (EPS) treated by combined ultrasound pretreatment and chemical re-flocculation on water treatment sludge settling performance. Chemosphere 170, 196-206.
6. Chen, C., Bin, L., Tang, B., Huang, S., Fu, F., Chen, Q., Wu, L., Wu, C., 2017b. Cultivating granular sludge directly in a continuous-flow membrane bioreactor with internal circulation. Chem. Eng. J. 309, 108–117.
7. Choi, J., Kim, E.S., Ahn, Y., 2017. Microbial community analysis of bulk sludge/cake layers and biofouling-causing microbial consortia in a full-scale aerobic membrane bioreactor. Bioresour. Technol. 227, 131–141.
8. Choo, K.H., Lee, C.H., 1996. Membrane fouling mechanisms in the membrane coupled anaerobic bioreactor. Water Res. 30, 1771–1780.
9. Cui, H., Yang, Y., Ding, Y., Li, D., Zhen, G., Lu, X., Huang, M., Huang, X., 2019. A novel pilot-scale tubular bioreactor enhanced floating treatment wetland (TB-EFTW) for efficient in-situ nitrogen removal from urban landscape water: long term performance and microbial mechanisms. Water Environ. Res. 19(11), 1498–1508.

10. Deng, L., Guo, W., Ngo, H.H., Mst. Zuthi, F.R., Zhang, J., Liang, S., Li, J., Wang, J., Zhang, X., 2015. Membrane fouling reduction and improvement of sludge characteristics by bioflocculant addition in submerged membrane bioreactor. Sep. Purif. Technol. 156, 450–458.

11. Deng, L., Guo, W., Ngo, H.H., Zhang, H., Wang, J., Li, J., Xia, S., Wu, Y., 2016. Biofouling and control approaches in membrane bioreactors. Bioresour. Technol. 221, 656–665.

12. Dogsa, I., Kriechbaum, M., Stopar, D., Laggnerz, P., 2005. Structure of bacterial extracellular polymeric substances at different pH values as determined by SAXS. Biophys. J. 83, 2711–2720.

13. Dong, J., Zhang, Z., Yu, Z., Dai, X., Xu, X., Alvarez, P.J.J., Zhu, L., 2017. Evolution and functional analysis of extracellular polymeric substances during the granulation of aerobic sludge used to treat p-chloroaniline wastewater. Chem. Eng. J. 330, 596–604.

14. Friha, I., Karray, F., Feki, F., Jlaiel, L., Sayadi, S., 2014. Treatment of cosmetic industry wastewater by submerged membrane bioreactor with consideration of microbial community dynamics. Int. Biodeter. Biodegradation 88, 125–133.

15. Gao, D.W., Wen, Z.D., Li, B., Liang, H., 2014. Microbial community structure characteristics associated membrane fouling in A/O-MBR system. Bioresour. Technol. 154, 87–93.

16. Gkotsis, P.K., Batsari, E.L., Peleka, E.N., Tolkou, A.K., Zouboulis, A.I., 2017. Fouling control in a lab-scale MBR system: Comparison of several commercially applied coagulants. J. Environ. Manage. 203, 838–846.

17. Gu, Y.Q., Li, T.T., Li, H.Q., 2018. Biofilm formation monitored by confocal laser scanning microscopy during startup of MBBR operated under different intermittent aeration modes. Process Biochem. 74, 132–140.

18. Huang, S., Shi, X., Bi, X., Lee, L.Y., Ng, H.Y., 2019. Effect of ferric hydroxide on membrane fouling in membrane bioreactor treating pharmaceutical wastewater. Bioresour. Technol. 292, 121852.

19. Inaba, T., Hori, T., Navarro, R.R., Ogata, A., Hanajima, D., Habe, H., 2018. Revealing sludge and biofilm microbiomes in membrane bioreactor treating piggery wastewater by non-destructive microscopy and 16S rRNA gene sequencing. Chem. Eng. J. 331, 75–83.

20. Ji, J., Li, J., Li, Y., Qiu, J., Li, X., 2015. Impact of modified starch on membrane fouling in MBRs. Desalination Water Treat. 57(24), 11008–11018.

21. Jia, S., Han, H., Zhuang, H., Hou, B., Li, K., 2015. Impact of high external circulation ratio on the performance of anaerobic reactor treating coal gasification wastewater under thermophilic condition. Bioresour. Technol. 192, 507–513.

22. Krzeminski, P., Iglesias-Obelleiro, A., Madebo, G., Garrido, J.M., van der Graaf, J.H.J.M., van Lier, J.B., 2012. Impact of temperature on raw wastewater composition and activated sludge filterability in full-scale MBR systems for municipal sewage treatment. J. Membr. Sci. 423–424, 348–361.

23. Lang, E., 2014. The Family *Kofleriaceae*. *In* Rosenberg, E., DeLong, E.F., Lory, S., Stackebrandt, E., and Thompson, F. (eds.), The Prokaryotes: *Deltaproteobacteria* and *Epsilonproteobacteria*, 183–189. Springer Berlin Heidelberg, Berlin, Heidelberg, Germany.

24. Layton, A.C., Karanth, P.N., Lajoie, A., Meyers, J., Gregory, I.R., Stapleton, R.D., Taylor, D.E., Sayler, G.S., 2000. Quantification of *Hyphomicrobium* Populations in Activated Sludge from an Industrial Wastewater Treatment System as Determined by 16S rRNA Analysis. Appl. Environ. Microbiol. 66(3), 1167–1174.

25. Li, X., Yang, S., 2007. Influence of loosely bound extracellular polymeric substances (EPS) on the flocculation, sedimentation and dewaterability of activated sludge. Water Res. 41, 1022–1030.

26. Liu, Y., Liu, Q., Li, J., Ngo, H.H., Guo, W., Hu, J., Gao, M., Wang, Q., Hou, Y., 2018. Effect of magnetic powder on membrane fouling mitigation and microbial community/composition in membrane bioreactors (MBRs) for municipal wastewater treatment. Bioresour. Technol. 249, 377–385.

27. Luo, J., Wei, L., Hao, T., Xue, W., Mackey, H.R., Chen, G.H., 2015. Effect of L-tyrosine on aerobic sludge granulation and its stability. RSC Adv. 5, 86513–86521.

28. Luo, G., Wang, Z., Li, Y., Li, J., Li, A.M., 2018. Salinity stresses make a difference in the start-up of membrane bioreactor: performance, microbial community and membrane fouling. Bioprocess and Biosyst. Eng. 42, 445–454.

29. Ma, C., Yu, S., Shi, W., Heijman, S.G.J., Rietveld, L.C., 2013. Effect of different temperatures on performance and membrane fouling in high concentration PAC–MBR system treating micro-polluted surface water. Bioresour. Technol. 141, 19–24.

30. Matar, G.K., Bagchi, S., Zhang, K., Oerther, D.B., Saikaly, P.E., 2017. Membrane biofilm communities in full-scale membrane bioreactors are not randomly assembled and consist of a core microbiome. Water Res. 123, 124–133.

518 31. Mateus, G.A.P., Formentini-Schmitt, D.M., Nishi, L., Fagundes-Klen, M.R.,
519 Gomes, R.G., Bergamasco, R., 2017. Coagulation/Flocculation with Moringa oleifera
520 and Membrane Filtration for Dairy Wastewater Treatment. Water Air Soil Pollut.
521 228(342), 1–13.
522 32. Miao, Y., Liao, R.H., Zhang, X.X., Wang, Y., Wang, Z., Shi, P., Liu, B., Li, A.M.,
523 2015. Metagenomic insights into Cr(VI) effect on microbial communities and
524 functional genes of an expanded granular sludge bed reactor treating high-nitrate
525 wastewater. Water Res. 76, 43–52.
526 33. Ngo, H.H., Guo, W.S., 2009. Membrane fouling control and enhanced phosphorus
527 removal in an aerated submerged membrane bioreactor using modified green
528 bioflocculant. Bioresour. Technol. 100, 4289–4291.
529 34. Park, P. Lee, C. Lee, S., 2006. Variation of specific cake resistance according to
530 size and fractal dimension of chemical flocs in a coagulation–microfiltration process.
531 Desalination 199, 213–215.
532 35. Peng, C., Gao, Y., Fan, X., Peng, P., Huang, H., Zhang, X., Ren, H., 2019.
533 Enhanced biofilm formation and denitrification in biofilters for advanced nitrogen
534 removal by rhamnolipid addition. Bioresour. Technol. 287, 121387.
535 36. Sutherland, I.W., 2001. Exopolysaccharides in biofilms, flocs and related structures.
536 Water Sci. Technol. 43(6), 77–86.
537 37. Tan, S., Cui, C., Chen, X., Li, W., 2017. Effect of bioflocculation on fouling-related
538 biofoulants in a membrane bioreactor during saline wastewater treatments. Bioresour.
539 Technol. 224, 285–291.

38. Xu, J., He, J., Wang, M., Li, L., 2018. Cultivation and stable operation of aerobic granular sludge at low temperature by sieving out the batt-like sludge. Chemosphere 211, 1219–1227.

39. Zhang, H., Sekiguchi, Y., Hanada, S., Hugenholtz, P., Kim, H., Kamagata, Y., Nakamura, K., 2003. *Gemmatimonas aurantiaca* gen. nov., sp. nov., a Gramnegative, aerobic, polyphosphate-accumulating micro-organism, the first cultured representative of the new bacterial phylum *Gemmatimonadetes* phyl. nov. Int. J. Syst. Evol. Microbiol. 53 (4), 1155-1163.

40. Zhang, H., Fan, X., Wang, B., Song, L., 2016. Calcium ion on membrane fouling reduction and bioflocculation promotion in membrane bioreactor at high salt shock. Bioresour. Technol. 200, 535–540.

41. Zhang, S., Zhou, Z., Li, Y., Meng, F., 2018. Deciphering the core fouling-causing microbiota in a membrane bioreactor: Low abundance but important roles. Chemosphere 195, 108–118.

42. Zhang, W., Jiang, F., 2019. Membrane fouling in aerobic granular sludge (AGS)-membrane bioreactor (MBR): Effect of AGS size. Water Res. 157, 445–453.

43. Zhao, Y., Jiang, B., Tang, X., Liu, S., 2019. Metagenomic insights into functional traits variation and coupling effects on the anammox community during reactor start-up. Sci. Total Environ. 687, 50–60.

44. Zheng, M., Zhu, H., Han, Y., Xu, C., Zhang, Z., Han, H., 2019. Comparative investigation on carbon-based moving bed biofilm reactor (MBBR) for synchronous removal of phenols and ammonia in treating coal pyrolysis wastewater at pilot-scale. Bioresour. Technol. 288, 121590.

563 45. Zhou, J.H., Wu, C.H., Cheng, G.F., Hong, Q.K, Li, Y.Z., Wang, H.Y., 2017a.
564 Impact of poly dimethyldiallylammonium chloride on membrane fouling mitigation in a
565 membrane bioreactor. Environ. Technol. 40(8), 1–7.
566 46. Zhou, J., Li, H., Chen, X., Wan, D., Mai, W., Sun, C., 2017b. Cometabolic
567 degradation of low-strength coking wastewater and the bacterial community revealed
568 by high-throughput sequencing. Bioresour. Technol. 245, 379–385.
569 47. Zhu, H., Han, Y., Ma, W., Han, H., Ma, W., 2017. Removal of selected nitrogenous
570 heterocyclic compounds in biologically pretreated coal gasification wastewater
571 (BPCGW) using the catalytic ozonation process combined with the two-stage
572 membrane bioreactor (MBR). Bioresour. Technol. 245, 786–793.

Table titles

Table 1. Fouling resistance distribution in the G-MBR and the CMBR

Table 2. SMP compositions, SMP concentrations, LB-EPS compositions and LB-EPS concentrations in the G-MBR and the CMBR at different TMP ranges

Table 1. Fouling resistance distribution in the G-MBR and the CMBR

Resistance distribution	G-MBR		CMBR	
	m^{-1}	% of R_T	m^{-1}	% of R_T
Total, R_T	3.73×10^{12}		6.13×10^{12}	
Cake layer, R_C	2.40×10^{12}	64.34	4.51×10^{12}	73.57
Pore blocking, R_P	0.17×10^{12}	4.56	0.46×10^{12}	7.50
Clean membrane, R_M	1.16×10^{12}	31.10	1.16×10^{12}	18.92

Table 2. SMP compositions, SMP concentrations, LB-EPS compositions and LB-EPS concentrations in the G-MBR and the CMBR at different TMP ranges

Concentration (mg/L)[a]	**TMP**					
	G-MBR			**CMBR**		
	< 10 kPa	**10-16 kPa**	**16-37 kPa**	**< 10 kPa**	**10-16 kPa**	**16-37 kPa**
SMP_C	5.33-10.78	12.34-17.36	23.76-29.26	9.06-15.26	27.36-30.18	32.39-53.67
SMP_P	9.24-18.65	22.37-26.73	29.36-33.72	11.41-24.32	20.76-25.68	28.79-42.18
SMP_P/SMP_C	1.57-2.09	1.54-1.81	1.15-1.24	1.26-1.59	0.76-0.85	0.79-0.89
Total SMP	14.82-29.43	34.71-44.09	53.12-62.98	20.47-39.58	48.12-55.86	61.18-95.85
$LB\text{-}EPS_C$	10.57-28.36	31.06-35.69	42.34-48.36	20.47-35.36	35.94-45.66	64.72-85.47
$LB\text{-}EPS_P$	33.23-59.26	63.75-68.71	70.69-75.36	42.22-63.96	64.62-75.39	72.71-95.37
$LB\text{-}EPS_P/LB\text{-}EPS_C$	2.09-3.14	1.93-2.05	1.56-1.67	1.81-2.06	1.65-1.80	0.89-0.90
Total LB-EPS	43.80-87.62	94.81-104.40	113.03-123.72	62.69-99.32	100.56-121.05	137.43-180.84

[a] $LB\text{-}EPS_C$, polysaccharides based LB-EPS; $LB\text{-}EPS_P$, proteins based LB-EPS; SMP_C, polysaccharides based SMP; SMP_P, proteins based SMP

Figure captions

Fig. 1. TMP profiles for the G-MBR and the CMBR

Fig. 2. Particle size distribution as particle volume fractions for the G-MBR (a) and the CMBR (b)

Fig. 3. The abundance of the major bacterial genera (top 30 most relative abundances in activated sludge of the G-MBR and the CMBR) at low TMP (< 10-16 kPa)

Fig. 4. The abundance of the major bacterial genera (top 35 most relative abundances in activated sludge of the G-MBR and the CMBR) at high TMP (> 35 kPa)

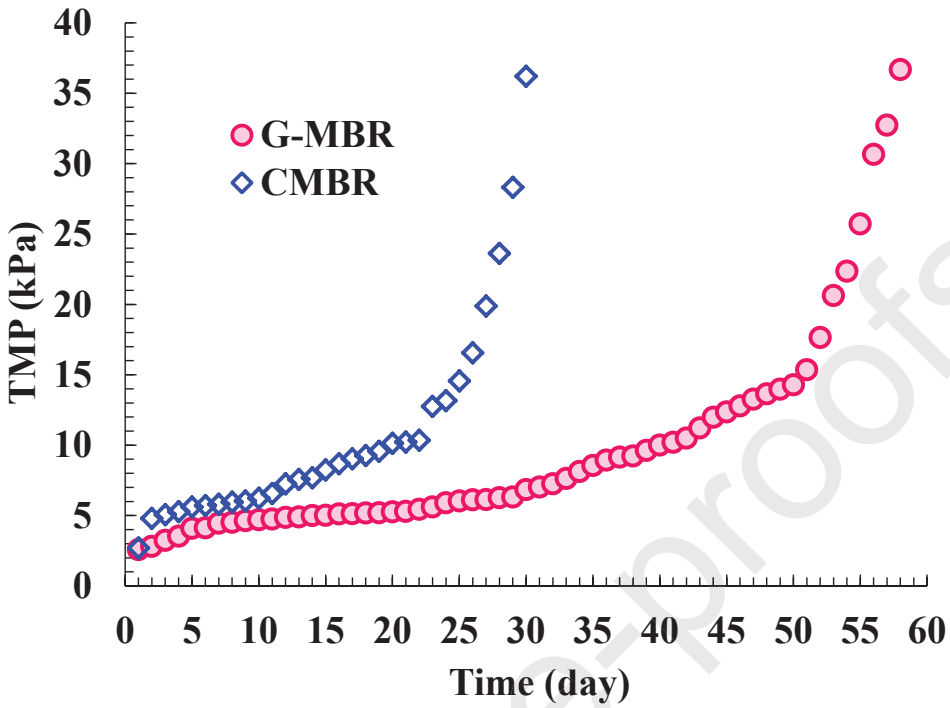

Fig. 1.

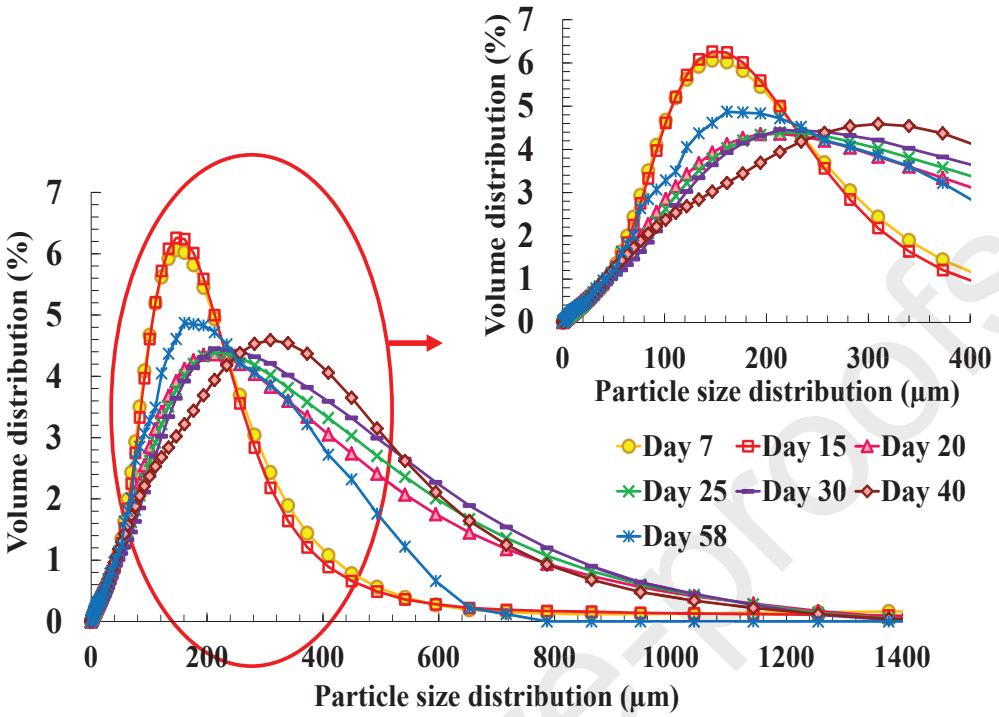
Volume distribution (%)
Particle size distribution (µm)
Day 7
Day 15
Day 20
Day 25
Day 30
Day 40
Day 58

(a)

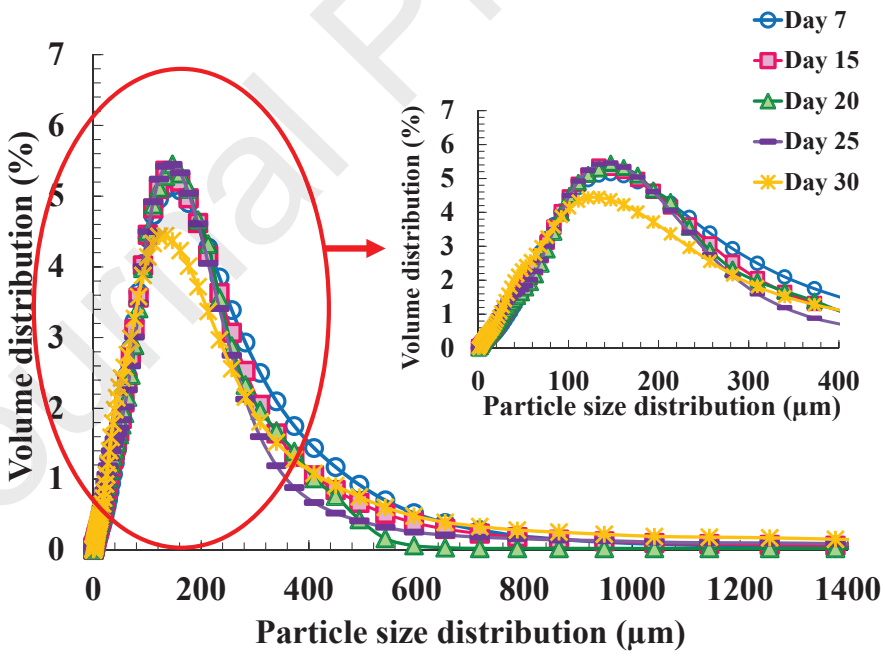
Volume distribution (%)
Particle size distribution (µm)
Day 7
Day 15
Day 20
Day 25
Day 30

(b)

Fig. 2.

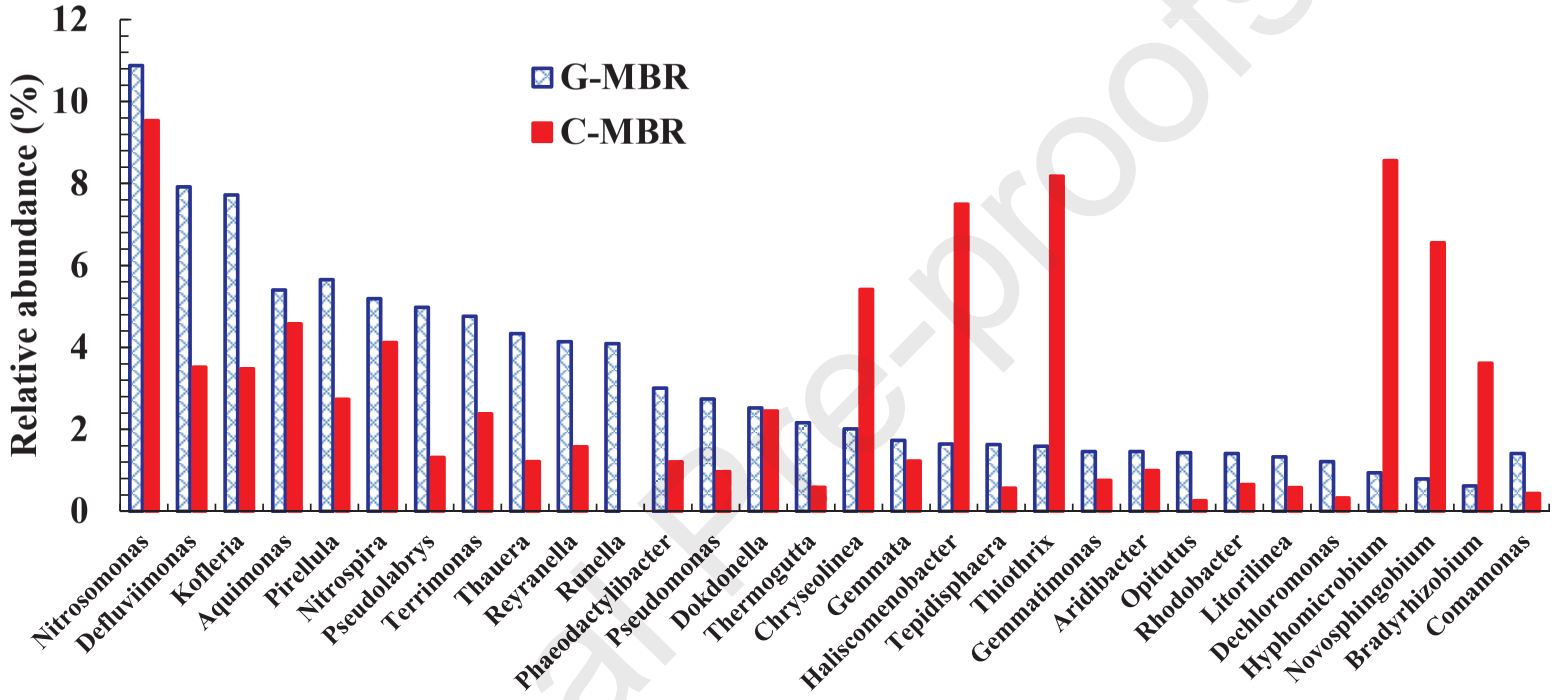

Fig. 3.

Fig. 4.